

# SnO<sub>2</sub> nanotubes with N-carbon coating for advanced Li-ion battery anodes

Junhai Wang<sup>1</sup>, Jiandong Zheng (✉)<sup>1</sup>, Liping Gao<sup>1</sup>, Chunyu Meng<sup>2</sup>,  
Jiarui Huang (✉)<sup>2</sup>, and Sang Woo Joo (✉)<sup>3</sup>

<sup>1</sup> School of Material and Chemical Engineering, Chuzhou University, Chuzhou 239000, China

<sup>2</sup> Key Laboratory of Functional Molecular Solids of the Ministry of Education, College of Chemistry and Materials Science, Anhui Normal University, Wuhu 241002, China

<sup>3</sup> School of Mechanical Engineering, Yeungnam University, Gyeongsan, Gyeongbuk 38541, Republic of Korea

E-mails: jrhuang@mail.ahnu.edu.cn (J.H.), zjd071@126.com (J.Z.), swjoo@yu.ac.kr (S.W.J.)

## Supplementary materials

### 1 Characterization

Scanning electron microscopy (SEM; S8100) with energy-dispersive X-ray spectroscopy (EDS) and high-resolution transmission electron microscopy (HRTEM; HT-7700) were performed to determine the morphologies and microstructures. The structure information and element valences were analyzed by X-ray diffraction (XRD; Bruker D8 Advance) using Cu K $\alpha$  radiation at a wavelength of 1.5418 Å and X-ray photoelectron spectroscopy (XPS; ESCALAB 250). The Raman spectra were conducted on a Renishaw in-Via spectrometer equipped with a 532 nm laser. Thermogravimetric analysis (TGA; SDT 2960) was used to analyze the SnO<sub>2</sub> and the carbon contents. The analysis was conducted from room temperature to 600 °C at a heating rate of 10 °C·min<sup>-1</sup> in air. The N<sub>2</sub> adsorption/desorption isotherms and pore size distribution were measured using the Brunauer–Emmett–Teller (BET) method (Micromeritics ASAP 2460).

### 2 Electrochemical measurements

CR2032 coin cells were used for the battery performance tests. Li-ion batteries (LIBs) were assembled in an argon-filled glove box ([O<sub>2</sub>] < 0.5 ppm, [H<sub>2</sub>O] < 0.5 ppm). The working electrodes were prepared by mixing SnO<sub>2</sub>@N-C nanotubes or SnO<sub>2</sub> nanotubes, acetylene black (conductive agent), and sodium carboxymethyl cellulose (CMC, binder) with a mass ratio of 8:1:1 with deionized water to produce the slurry. The copper foil was coated evenly with the slurry and dried in a vacuum oven at 60 °C for 24 h. The electrodes were pressed into a disc ( $d = 12$  mm). The mass loading of the active mass among SnO<sub>2</sub>/N-C NT and SnO<sub>2</sub> NT anodes were approximately 1.89 and 1.85 mg·cm<sup>-2</sup>, respectively. The counter electrode was a lithium sheet with a polypropylene film (Celgard 240) as the separator. 1 mol·L<sup>-1</sup> LiPF<sub>6</sub> dissolved in carbonate/diethyl carbonate, ethylene carbonate/dimethyl with 1:1:1 (volume ratio) was used as the electrolyte. All cells were tested using a galvanostatic discharge/charge cycle test on a battery test instrument (Shenzhen Neware

Technology Co., Ltd., CT-4008) at different current densities from 0.01 to 3.0 V (vs. Li/Li<sup>+</sup>) at room temperature. Cyclic voltammetry (CV) was performed on an electrochemical workstation (CHI-660D) at different scan rates between 0.01 to 3.0 V (vs. Li/Li<sup>+</sup>). The impedance measurements were carried out by applying an AC amplitude of 5 mV<sub>rms</sub> on an equilibrium potential of 2.4 V (vs. Li/Li<sup>+</sup>) over the frequency range of 10 mHz to 100 kHz.

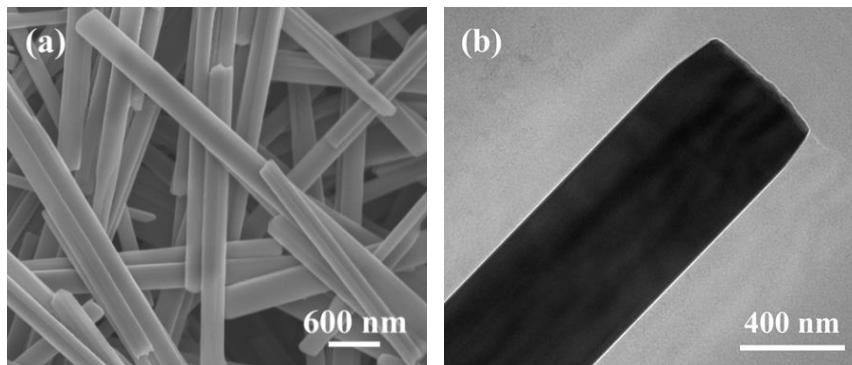


**Fig. S1** (a) SEM and (b) TEM images of MoO<sub>3</sub> nanorods.

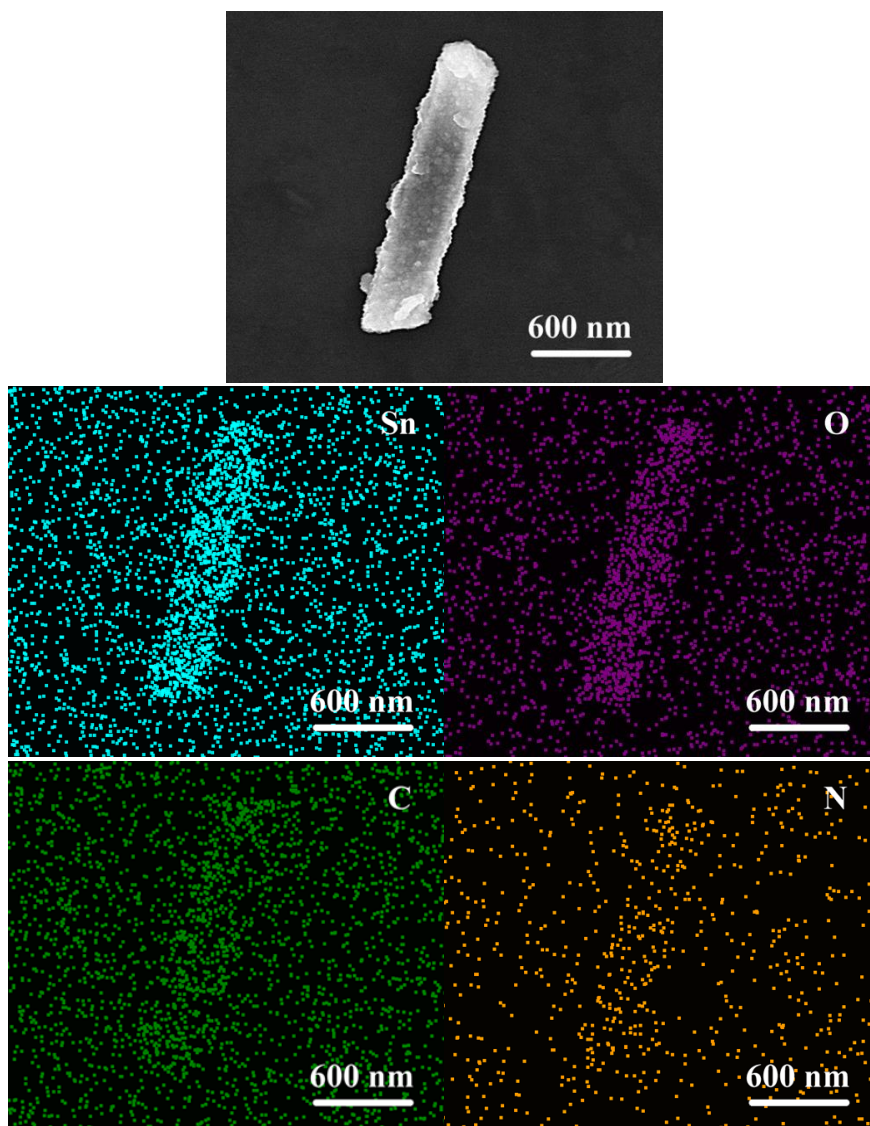


**Fig. S2** Elemental mapping images of SnO<sub>2</sub>@N-C NT.

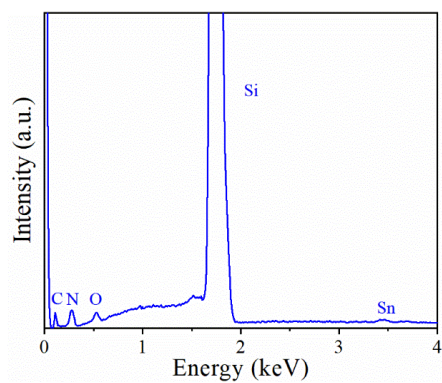


**Fig. S3** EDS analysis of SnO<sub>2</sub>@N-C NT.

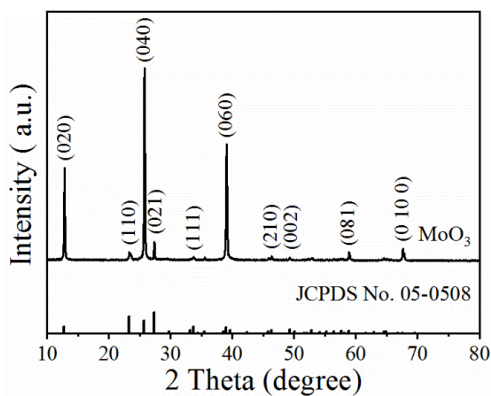


**Fig. S4** XRD pattern of MoO<sub>3</sub> nanorods.

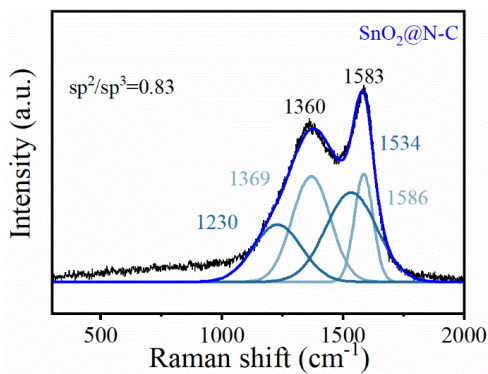


**Fig. S5** Deconvoluted Raman spectra of D and G bands.

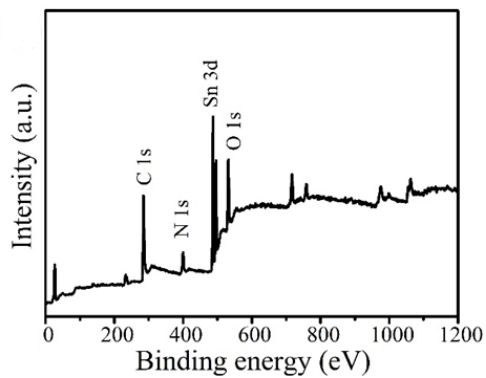


**Fig. S6** XPS survey spectrum of SnO<sub>2</sub>@N-C NTs.

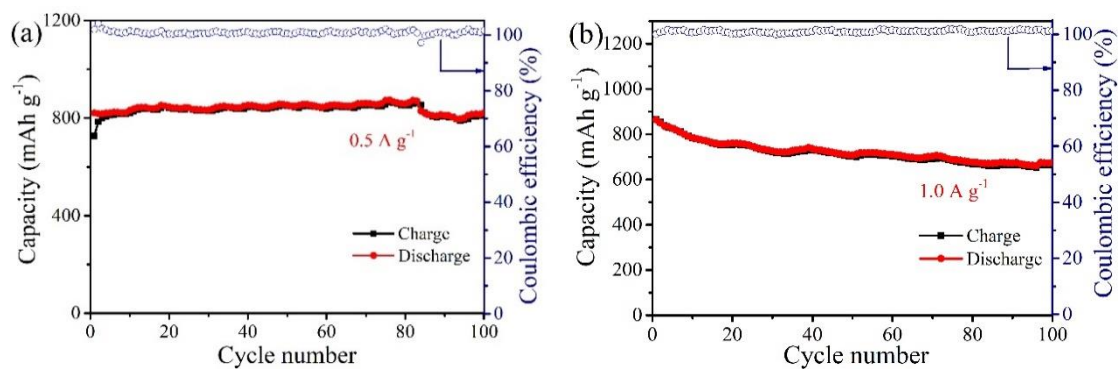


**Fig. S7** Cycling stability of SnO<sub>2</sub>@N-C NT anodes at current densities of (a) 0.5 A·g<sup>-1</sup> and (b) 1.0 A·g<sup>-1</sup>.

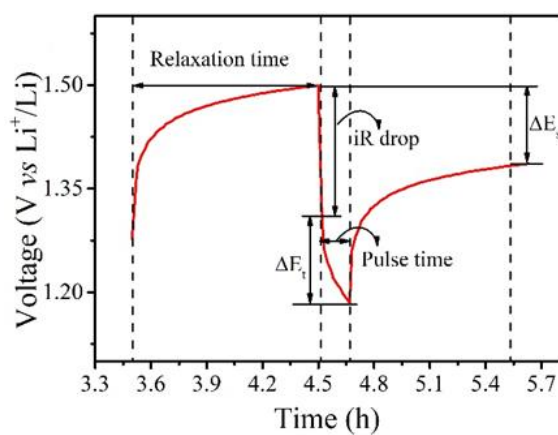


**Fig. S8** Voltage response over time during a single current pulse.

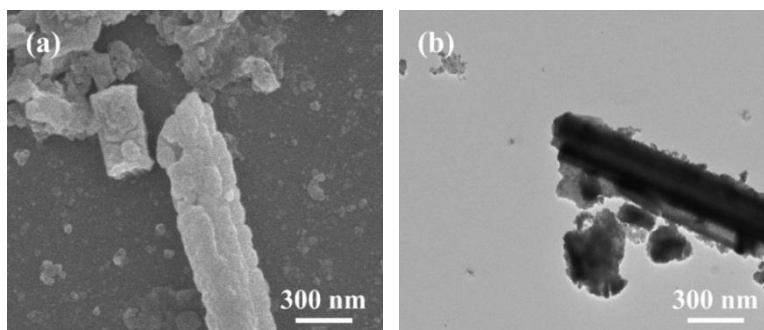


**Fig. S9** (a) SEM and (b) TEM images of the SnO<sub>2</sub>@N-C NT electrode after 100 cycles.

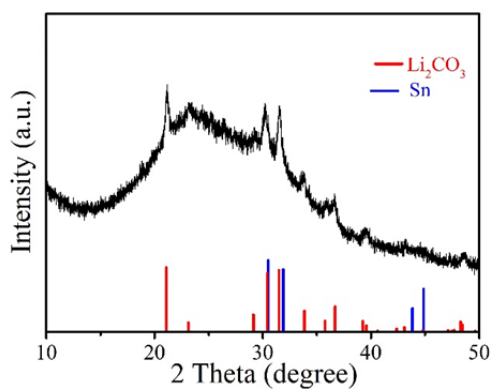


**Fig. S10** XRD pattern of the SnO<sub>2</sub>@N-C NT electrode after 100 cycles.

**Table S1** Comparison of cyclic properties between synthetic materials and some other composites reported in literature

Electrode material	Current density/(A·g <sup>-1</sup> )	Cycle number	Reversible capacity/(mAh·g <sup>-1</sup> )	Ref.
SnO <sub>2</sub> microspheres	0.1	50	760.0	[38]
Co-SnO <sub>2</sub> @GO nanosheets	0.1	90	1157.4	[39]
SnO <sub>2</sub> @C nanowires	0.1	50	680.0	[40]
SnO <sub>2</sub> @SnS <sub>2</sub>	0.1	50	1068.0	[41]
SnO <sub>2</sub> @FeOOH@C	1.0	160	262.2	[42]
SnO <sub>2</sub> @PPy	1.0	100	591.0	[43]
SnO <sub>2</sub> @MnO <sub>2</sub> @GO	1.0	100	400.0	[44]
CoPPc@SnO <sub>2</sub> nanotubes	0.2	400	950	[17]
SnO <sub>2</sub> @N-C nanotubes	0.1	100	1369.3	this work
	1.0	100	622.8	this work

**Table S2** Simulation model with the estimated values

$R/\Omega$	$R_1$	$R_2$	$R_{ct}$
SnO <sub>2</sub> @N-C NT (fresh cell)	1.7	–	98.9
SnO <sub>2</sub> @N-C NT (after 100 cycles)	3.7	3.7	11.4
SnO <sub>2</sub> NT (fresh cell)	1.6	–	279.1
SnO <sub>2</sub> NT (after 100 cycles)	8.7	58.7	44.2